

Influence of steel fiber and reinforcing details on the ultimate bearing strength of the post-tensioning anchorage zone

Jin-Kook Kim^{1a}, Jun-Mo Yang^{*1} and Yangsu Kwon^{2b}

¹Steel Structure Research Group, POSCO, 100, Songdogwahak-ro, Yeonsu-gu, Incheon, 21985, Republic of Korea

²Site & Structural Engineering Group, KHNP Central Research Institute, 70, 1312-gil, Yuseong-daero, Yuseong-gu, Daejeon, 34101, Republic of Korea

(Received February 15, 2016, Revised May 24, 2016, Accepted May 25, 2016)

Abstract. In this paper, the effects of steel-fiber and rebar reinforcements on the ultimate bearing strength of the local anchorage zone were investigated based on experiments and comparisons between test results and design-equation predictions (AASHTO 2012, NCHRP 1994). Eighteen specimens were fabricated using the same anchorage device, which is one of the conventional anchorage devices, and two transverse ribs were used to secure an additional bearing area for a compact anchorage-zone design. Eight of the specimens were reinforced with only steel fiber and are of two concrete strengths, while six were reinforced with only rebars for two concrete strengths. The other four specimens were reinforced with both rebars and steel fiber for one concrete strength. The test and the comparisons between the design-equation predictions and the test results showed that the ultimate bearing strength and the section efficiency are highly affected by the reinforcement details and the concrete strength; moreover, the NCHRP equation can be conservatively applied to various local anchorage zones for the prediction of the ultimate bearing strength, whereby conditions such as the consideration of the rib area and the calibration factor are changed.

Keywords: post-tension; anchorage; bearing strength; steel fiber; local anchorage zone

1. Introduction

The creation of pre-stressed concrete structures through post-tensioning requires the use of an anchorage device so that large tendon forces can be introduced into the structural members. The transfer of the tendon forces is localized and this causes high compressive stresses immediately ahead of the anchorage. The region around the anchorage affected by the introduction of the tendon forces is called the “local anchorage zone” or “local zone.” Frequently, proprietary special anchorages comprising additional ribs for the increment of the bearing area are used in pre-stressed concrete structures, and the specified, local confinement reinforcements that are employed for each anchorage device carry bearing stresses that are higher than the cylinder strength of the

*Corresponding author, Senior Researcher, E-mail: junrhkd@gmail.com

^aPrincipal Researcher

^bAssistant Research Engineer

concrete. The use of such anchorages should be based on an acceptance test (called a “load transfer test”) that proves that such high bearing stresses do not cause failure and satisfy the serviceability.

A number of tests were conducted by Komendant (1952), who used plain concrete blocks with a number of bearing plates, and the results are the basis of the proposal regarding the square-root formula of the ultimate bearing strength of a concrete block, which is still used by ACI (ACI 318-14 2014), albeit with some modifications. Later, numerous researchers verified the formula and proposed a number of modifications (Niyogi 1974, Suzuki *et al.* 1982); for instance, alterations in consideration of the effects of reinforcement confinement. Suzuki *et al.* (1982) also found the following three failure modes from the test results: (1) splitting of the cylinder for unreinforced or lightly reinforced specimens; (2) complete crushing of concrete at the local zone; (3) failure of concrete beneath the spiral with the formation of a concrete cone that leads to a splitting of the concrete below. Wurm and Daschner (1977) found that there is an upper limit when the confinement effect is used for strengthening. Roberts (1990) proposed a design equation for the ultimate bearing strength of the local zone, which is based on the work of Richart *et al.* (1928) and is in consideration of the confinement effect, and suggested a confining-pressure limit of 8.27 MPa based on the results of Wurm and Daschner (1977). Cervenka and Ganz (2014) conducted an analytic and experimental study on the anchorage zone using VSL anchorage devices. The study yielded the following findings: (1) The NCHRP design equation could be suitably calibrated for the test results. (2) The NCHRP design equation underestimated the real resistance in the case of rectangular cross-sections, but overestimated it in the case of square sizes larger than the minimum anchorage spacing. (3) The NCHRP design model should not be applied for cases that have not been confirmed by testing. The focus of all of the previous research efforts is an exact prediction of the ultimate bearing capacity of the anchorage zone and its failure mode. So far, the NCHRP design equation provides a reasonably accurate prediction.

Regarding recent designs, high-strength concrete with a slender concrete section is typically used, as an efficient, small anchorage zone is required and a dense rebar reinforcement around the anchorage device eventuates. A dense reinforcement, however, deteriorates the workability of the design, and sometimes even the construction quality. In this paper, the effects of steel-fiber and rebar reinforcements on the ultimate bearing strength of the local anchorage zone was investigated based on experiments and comparisons between test results and design-equation predictions (AASHTO 2012, NCHRP 1994). Eighteen specimens were fabricated using the same anchorage device, which is one of the conventional anchorage devices, and two transverse ribs were used to secure an additional bearing area for a compact anchorage-zone design. Eight of the specimens were reinforced with only steel fiber and are of two concrete strengths, while six of them were reinforced with only rebars for two concrete strengths. The other four specimens were reinforced with both rebars and steel fiber for a single concrete strength. From an analysis of the test results, the sectional efficiency was investigated according to the reinforcements of steel fiber and rebar and the concrete strength. Based on the comparisons between the design-equation predictions and the test results, an efficient and safe method for the application of an anchorage-zone design equation regarding each specimen group was proposed.

2. Experimental study

2.1 Specimens

Eighteen specimens were fabricated. Eight of them, grouped as “SF,” were reinforced with only steel fiber for two types of design-concrete strength. Six of the specimens, grouped as “RC,” were reinforced with only steel rebars, also for two types of design-concrete strength. The variable of the RCs is local reinforcement, whereby a spiral-based lateral confinement was achieved. The other four specimens, grouped as “RC-SF,” were reinforced with both steel rebars and steel fiber, and a local-reinforcement variable also applied for this group. The details of the test specimens can be found in Table 1. The section of the specimen is square and the height is twice the size of the side length (B). All of the specimens share the same anchorage in the concrete that accommodates 15 pre-stressing strands of a 333 kN tensile strength. The 333 kN, which is a minimum tensile load of strand with ultimate strength of 2,400 MPa, is specified in KS D 7002 (2011). The strands having an ultimate tensile strength of 2400 MPa have recently been developed, and experimental studies have been performed to verify the suitability of the strands, such as the mechanical properties or stress-strain relationship (Kim *et al.*, 2013). The anchorage comprises two transverse ribs for an additional bearing area. A representative drawing of the specimens including the anchorage can be seen in Fig. 1.

2.2 Material properties

Three types of steel rebars were used in the construction of the test specimens. All of the steel

Table 1 Details of test specimens

No.	Specimens	B (mm)	$f_{ci}/f_i/f_{i,eq}$ (MPa)	S.F. (%)	Spiral	Stirrup	f_{lat} (MPa)
1	SF-430-50-1	430	50.3/7.1/2.1	0.38 %	-	-	-
2	SF-430-50-2	430	44.4/7.0/1.9	0.38 %	-	-	-
3	SF-430-50-3	430	58.0/6.9/2.1	0.38 %	-	-	-
4	SF-430-50-4	430	49.7/ 8.2/2.8	0.38 %	-	-	-
5	SF-360-70-5	360	75.1/7.4/1.8	0.38 %	-	-	-
6	SF-360-70-6	360	69.1/7.5/1.4	0.38 %	-	-	-
7	SF-360-70-7	360	74.5/7.6/2.2	0.38 %	-	-	-
8	SF-360-70-8	360	69.1/7.3/1.5	0.38 %	-	-	-
9	RC-430-35-1	430	34.2/ - / -	-	D16-8@50	D13-8@50	9.69
10	RC-430-35-2	430	34.2/ - / -	-	D13-9@50	D13-6@75	6.18
11	RC-430-35-3	430	35.7/ - / -	-	D16-9@50	D16-9@50	9.13
12	RC-430-65-1	430	63.9/5.1/0.1	-	D16-9@50	D16-9@50	9.13
13	RC-430-65-2	430	63.9/5.1/0.1	-	D13-9@50	D13-9@50	5.83
14	RC-430-65-3	430	63.9/5.1/0.1	-	D10-9@50	D10-9@50	3.28
15	RC-SF-430-55-1	430	54.6/7.3/6.5	0.50 %	D13-9@50	D13-9@50	5.83
16	RC-SF-430-55-2	430	54.6/7.3/6.5	0.50 %	D10-9@50	D10-9@50	3.28
17	RC-SF-430-55-3	430	54.6/7.3/6.5	0.50 %	D16-6@75	D16-6@75	6.09
18	RC-SF-430-55-4	430	54.6/7.3/6.5	0.50 %	D16-5@100	D16-5@100	4.57

- The lateral spiral-confinement pressure is defined as $f_{lat} = \frac{2A_s f_y}{D_{sp} \cdot s}$

- The external diameters of the spirals, D_{sp} , from No. 9 to No. 10 and from No. 11 to No. 18 are 328 mm and 348 mm, respectively.

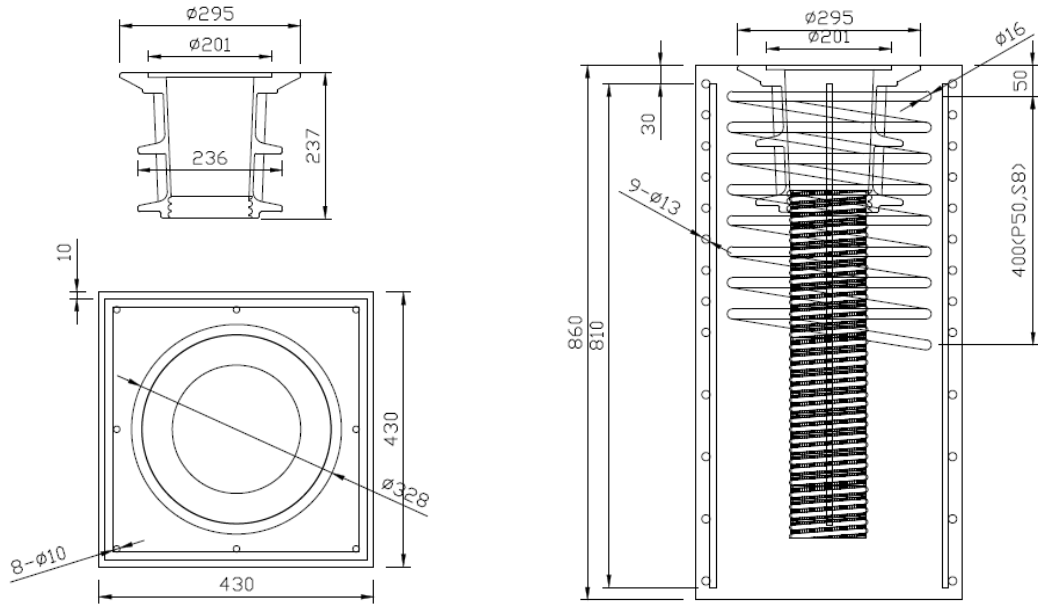


Fig. 1 Representative drawings of specimen (RC-430-35-1)

Table 2 Properties of steel rebars

Designation	Nominal diameter (mm)	Nominal cross-sectional area (mm ²)	Nominal tensile strength (MPa)	Nominal yield strength (MPa)
D10	9.53	71.3	560	400
D13	12.7	126.7	560	400
D16	15.9	198.6	560	400

Table 3 Properties of hooked-end steel fibers

Specimens	l_f (mm)	Dimension (mm ²)	l_f/d_f	Tensile strength (MPa)	Ultimate elongation (%)
No. 1 to No.8	30.0	Φ 0.50	60.0	1195.5	0.60
No. 15 to No. 18	35.0	Φ 0.55	63.6	1444.6	0.72

rebars satisfied the specifications listed in KS D 3504 (2011), and the nominal data that are presented in Table 2 were used for the design of the test specimens. Bundle-type, hooked-steel fibers were added to the steel-fiber-reinforced concrete specimens, and the two types of steel-fiber properties, which were supplied by the manufacturer, are presented in Table 3.

The specimens were fabricated using normal-weight concrete with the design strengths of each of the specimens. The second-to-last letter in the specimen name is the design-compressive strength of the concrete. All eight SF specimens, from No. 1 to No. 8, were fabricated using different batches of concrete on different days; meanwhile, the other specimens were fabricated using the same batches of concrete for each of the series of the RC-430-35, RC-430-65, and RC-SF specimens. Ordinary portland cement and ground-granulated, blast-furnace slag were used and mixed as a cementitious material, and a chemical admixture of the polycarboxylic-acid, high-range-AE, water-reducing agent was used to acquire the properties of the fresh concrete.

The material properties of the concrete were obtained on the day that each of the specimens was tested and are summarized in Table 1. Standard compressive-cylinder tests for which 100 mm-diameter×200 mm-high cylinders were used were conducted to determine the mean values of the concrete-compressive strength, f_{ci} . For the steel-fiber-reinforced concrete, the first-peak flexural tensile strength, f_i ; the equivalent flexural tensile strength, $f_{t,eq}$; and the load-versus-deflection curve shown in Fig. 2 were obtained from the third-point loading tests on 100 mm×100 mm×350 mm flexural beams, which are defined in ASTM C 1609 (2012). The equivalent flexural tensile strength, $f_{t,eq}$, is calculated as follows

$$f_{t,eq} = T_{150}^D \frac{150}{bd^2}, \tag{1}$$

where, T_{150}^D is the total area under the load-deflection curve up to a net deflection of $l/150$ (=2 mm) of the span length (ASTM International 2012).

As shown in Table 1 and Fig. 2, the toughness of the concrete of the RC-SF specimens is two to four times higher than that of the SF specimens, while the flexural tensile strength is of an equivalent value; this is because the aspect ratio, tensile strength, and volume percentage of the steel fibers that are used in the RC-SF specimens are higher than those used in the SF specimens. The parameters of aspect ratio, tensile strength, and volume percentage are the main factors for determining the toughness of fiber-reinforced concrete. In this case, the compressive strength of the fiber-reinforced concrete did not impact the equivalent tensile strength and toughness of the concrete at all.

The toughness-performance-level method proposed by Morgan *et al.* (1995) was also used to determine the toughness of the fiber-reinforced concrete. As shown in Fig. 2, the toughness-performance levels of the concretes of the SF specimens and RC-SF specimens are II and IV, respectively.

2.2 Test procedure

The load-transfer test was conducted in accordance with ETAG 013 (EOTA, 2002). During the load-transfer test, the specimen was mounted on a 10MN UTM (universal test machine). The load was applied to the anchor head that is placed on the top of the anchorage, thereby simulating the loading condition of a complete anchorage. The load was increased up to 80% of the nominal

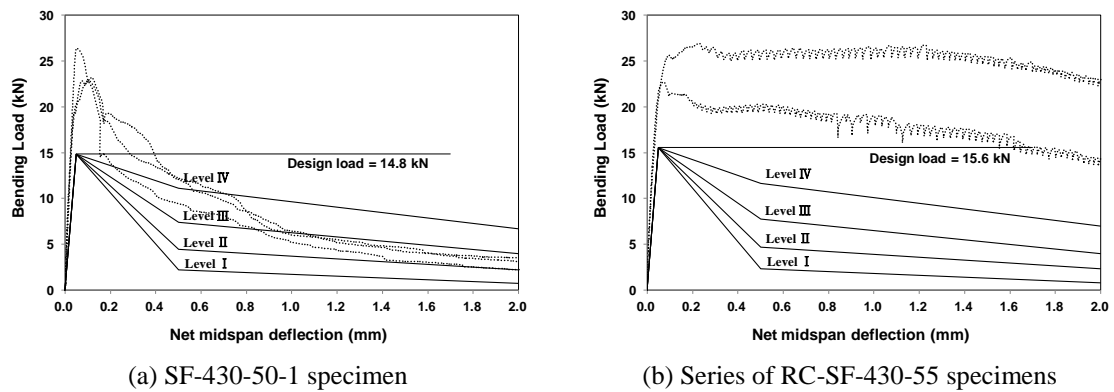


Fig. 2 Load-deflection curve and flexural-toughness-performance level of the fiber-reinforced concrete

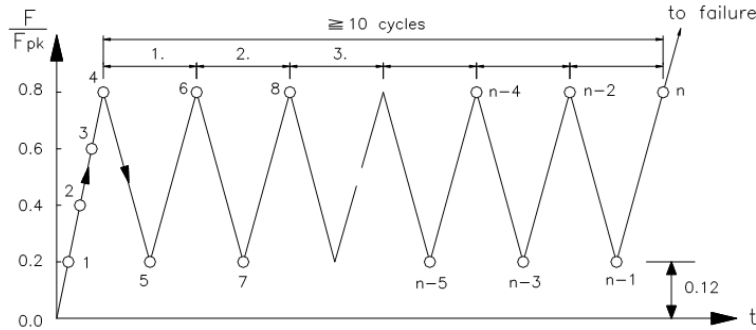


Fig. 3 Procedure of load-transfer test (EOTA 2002)

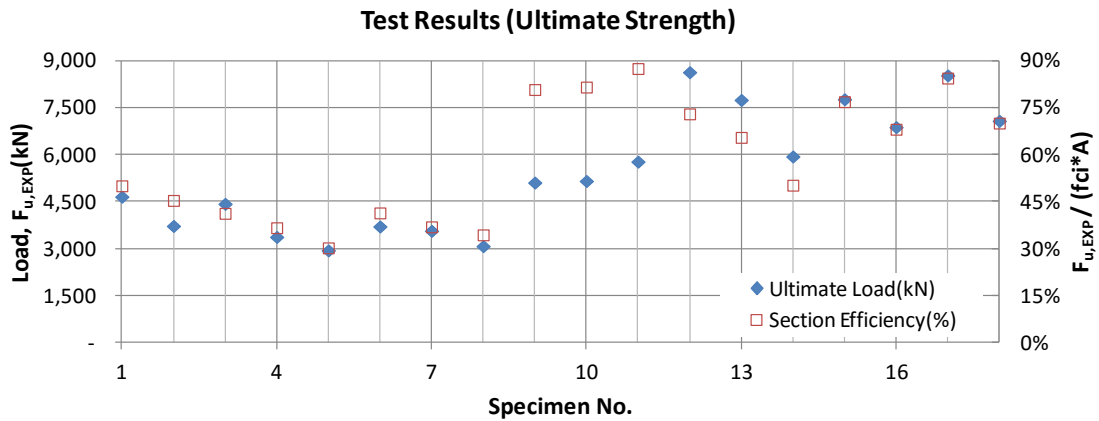


Fig. 4 Ultimate bearing strengths and section efficiencies of specimens

strength of the tendon (F_{pk}). After reaching the load of $0.8 F_{pk}$, at least 10 slow load cycles were performed, with $0.8 F_{pk}$ and $0.12 F_{pk}$ being the upper and the lower load limits, respectively. The load was then applied up to the point of failure, as seen in Fig. 3 (EOTA 2002). In ETAG013 (EOTA 2002), longitudinal and transverse strain measurements are used to assess stabilization criteria. However, strain measurements are excluded in this paper because this paper focused on the ultimate bearing strength of each specimen.

3. Test results and discussions

The results of the load-transfer test and the section efficiencies are presented in Table 4 and Fig. 4. The section efficiency is defined as the ratio of the load-transfer-test results, $F_{u,EXP}$, to the gross section strength, $f_{ci}A$, for the comparison with the test results. While all of the specimens were fabricated with the same anchorage, meaning that all of the corresponding required ultimate strengths are the same, the section efficiencies of the specimens are different due to the variables of the concrete strength and the reinforcing detail. For the ultimate strength, the RC-430-65-1 and RC-SF-430-55-3 specimens showed the highest strengths, and the series of the RC-430-65 and RC-SF-430-55 specimens (referred to as “RC-430-65s” and “RC-SF-430-55s”) showed strengths

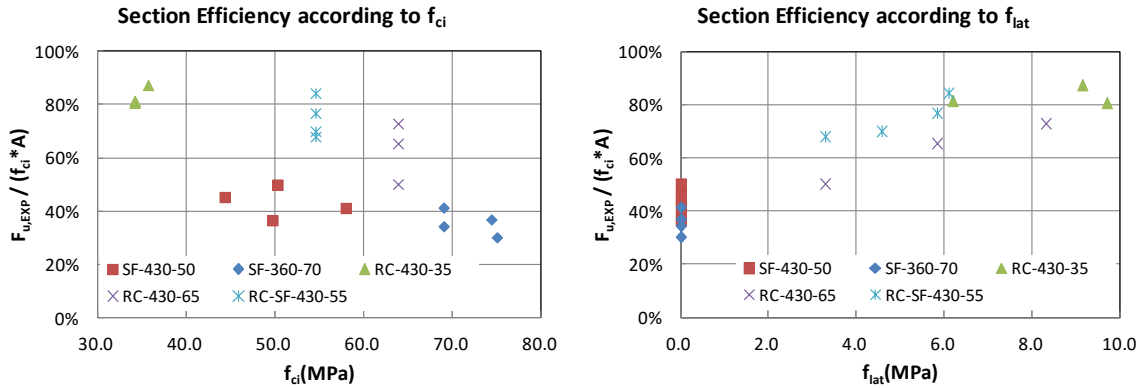
Table 4 Test results and section efficiencies

No.	Specimens	$F_{u,EXP}$ (kN)	$F_{u,EXP} / (f_{ci} \cdot A)$ (%)
1	SF-430-50-1	4,662	50 %
2	SF-430-50-2	3,728	45 %
3	SF-430-50-3	4,434	41 %
4	SF-430-50-4	3,378	37 %
5	SF-360-70-5	2,949	30 %
6	SF-360-70-6	3,712	41 %
7	SF-360-70-7	3,572	37 %
8	SF-360-70-8	3,085	34 %
9	RC-430-35-1	5,113	81 %
10	RC-430-35-2	5,163	82 %
11	RC-430-35-3	5,781	88 %
12	RC-430-65-1	8,637	73 %
13	RC-430-65-2	7,750	66 %
14	RC-430-65-3	5,946	50 %
15	RC-SF-430-55-1	7,772	77 %
16	RC-SF-430-55-2	6,883	68 %
17	RC-SF-430-55-3	8,532	84 %
18	RC-SF-430-55-4	7,082	70 %

that are larger overall than those of the other specimens. The series of the SF specimens (referred to as “SFs”) showed much lower strengths than the others. Regarding efficiency, RC-430-35s showed the highest efficiencies, followed by RC-SF-430-55s. A high ultimate bearing strength, or the load-transfer capacity from the anchorage to the concrete, can be achieved using both high-strength concrete and a large amount of rebar reinforcement. Notably, efficiency has a positive relationship with reinforcement but a negative relationship with the concrete strength.

The emphasis of the review of the section efficiency is the concrete strength and the lateral spiral-confinement pressure, as shown in Fig. 5. In Fig. 5(a), it is clear that, as the concrete strength increased, the section efficiency decreased and the effect on the rebar-reinforced specimens is more significant than that regarding the specimens reinforced with only steel fiber. In addition, among the high-strength-concrete specimens reinforced with rebars, a lesser number of reinforced specimens, such as RC-430-65-2, RC-430-65-3, RC-SF-430-55-2, and RC-SF-430-55-4, showed drastic section-efficiency declines; therefore, high-strength concrete can be effectively used only with an appropriate rebar reinforcement. Additionally, while the confining pressure of RC-430-35-1 is larger than those of the others in the same group, its efficiency is the lowest; this is attributed to the depth of the spiral, which is lower than the others, and it resulted in the earlier failure of the concrete near the end of the spiral. These results indicate that the reinforcing details, rather than the concrete strength, exert a greater influence over the section efficiency.

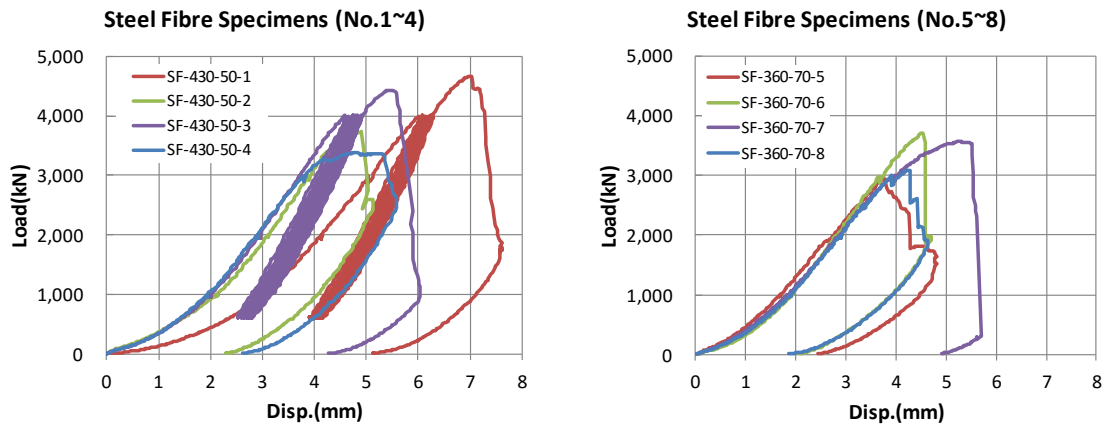
In the test results, the maximum section efficiency occurs at a value between 80% and 90%, and the confinement influence appeared to converge, as seen in Fig. 5(b), even though the convergence depends on variables such as the concrete strength and the addition of steel fiber. For the specimens reinforced with only rebars, the threshold seems to be between lateral confinement



(a) Effect of concrete compressive strength

(b) Effect of spiral-confinement pressure

Fig. 5 Section efficiencies of specimens according to design variables



(a) Specimens No. 1 to No. 4

(b) Specimens No. 5 to No. 8

Fig. 6 Load-displacement curves of load-transfer tests for specimens reinforced with only steel fiber

pressures of 6 MPa and 9 MPa, which is similar to Roberts (1990)'s conclusion; however, for the specimens reinforced with both rebars and steel fiber, the threshold appears to be around 6 MPa. It is therefore possible to determine that the threshold of the spiral-confinement pressure is between 6 MPa and 9 MPa, irrespective of the concrete strength and the addition of steel fiber.

3.1 Specimens reinforced with only steel fiber

Fig. 6 and Fig. 7 show the load-displacement curves of the load-transfer test and the failure modes for the specimens reinforced with only steel fiber. All of the 70 MPa specimens and two of the 50 MPa specimens could not reach the upper load ($0.8 F_{pk}$) of the cyclic load, and all of the specimens showed a brittle failure from a sudden drop of the load-displacement curve after the peak point. The high-strength specimens, SF-360-70s, showed ultimate strengths that are 18 % lower on average than those of SF-430-50s, even though the gross section strengths are similar. It

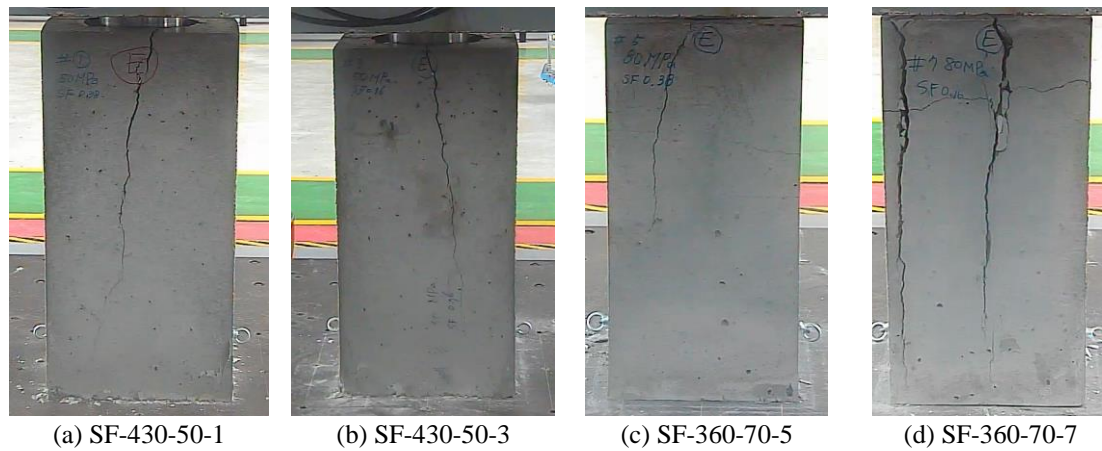


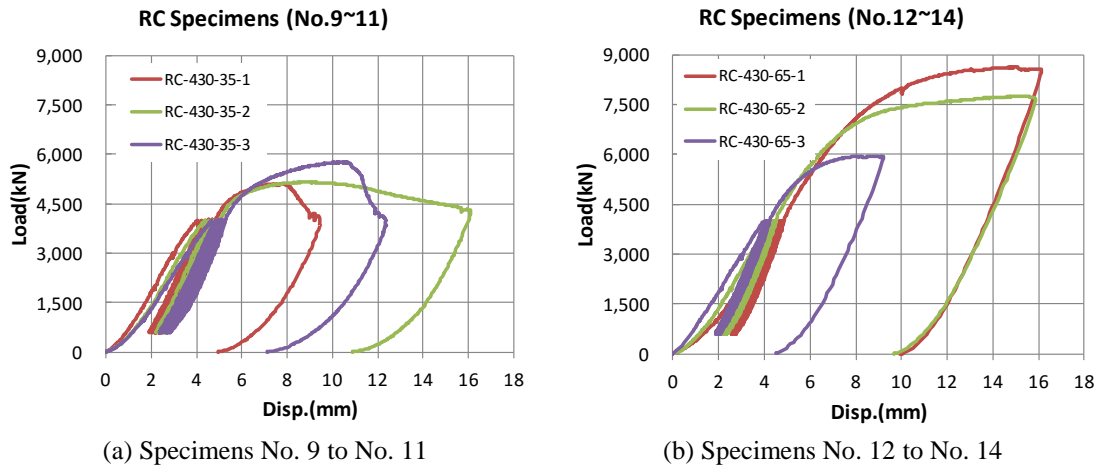
Fig. 7 Failure modes of specimens reinforced with only steel fiber

is possible to explain that the relatively larger section loss of the smaller specimens that is due to the duct results in a lesser confinement by the surrounding concrete. All of the failure modes are considered split fractures that are governed by a bursting force, revealing that the confinement and bursting capacity of the steel fiber alone are insufficient for the local post-tensioning anchorage zone when the equivalent flexural tensile strength of the steel-fiber-reinforced concrete is less than 2.8 MPa; furthermore, it seems that a relation does not exist between the ultimate strength of the load-transfer tests and the tensile properties of the steel-fiber-reinforced concrete under this design condition. To determine whether the toughness of the steel-fiber-reinforced concrete is higher, extensive studies might be required.

3.2 Specimens reinforced with only steel rebars

Fig. 8 and Fig. 9 show the load-displacement curves of the load-transfer test and the failure modes for the specimens reinforced with only steel rebars. The behavior of the No. 9 specimen (RC-430-35-1) in Fig. 8(a) is brittle compared with those of the No. 10 and No. 11 specimens; this can also be explained by the effect of a lesser spiral depth. It seems that the spiral could not cover the entire local zone that is affected by the stress concentration near the anchorage device. The comparison of the curves in Fig. 8(a) demonstrates that appropriate reinforcement coverage and the spiral depth determine the higher strength and ductility of the anchorage zone. RC-430-35-2 showed a higher strength and ductility in spite of a lesser confinement, and a spiral of a larger diameter and greater depth resulted in the highest strength of RC-430-35-3.

Meanwhile, the results of RC-430-65s indicate that the ultimate bearing strengths and corresponding displacements are proportional to the confinement pressure, and that this is due to the fact that the design of the specimens, with the exception of the confinement pressure, comprises an identical geometry. The specimens were reinforced with stirrups along with the spiral to control any cracking and to prevent a bursting failure; consequently, many cracks appeared on the concrete surfaces. A different failure mode was observed for the SFs, as specimens in this group seem to fail through a complete crushing of the concrete at the local zone, or a failure of the concrete beneath the spiral due to the formation of a concrete cone that splits the concrete below, as seen in Fig. 9. The minimum stirrup reinforcements in the specimens, D10-9@50, could



(a) Specimens No. 9 to No. 11 (b) Specimens No. 12 to No. 14
 Fig. 8 Load-displacement curves of load-transfer tests for specimens reinforced with only steel rebars

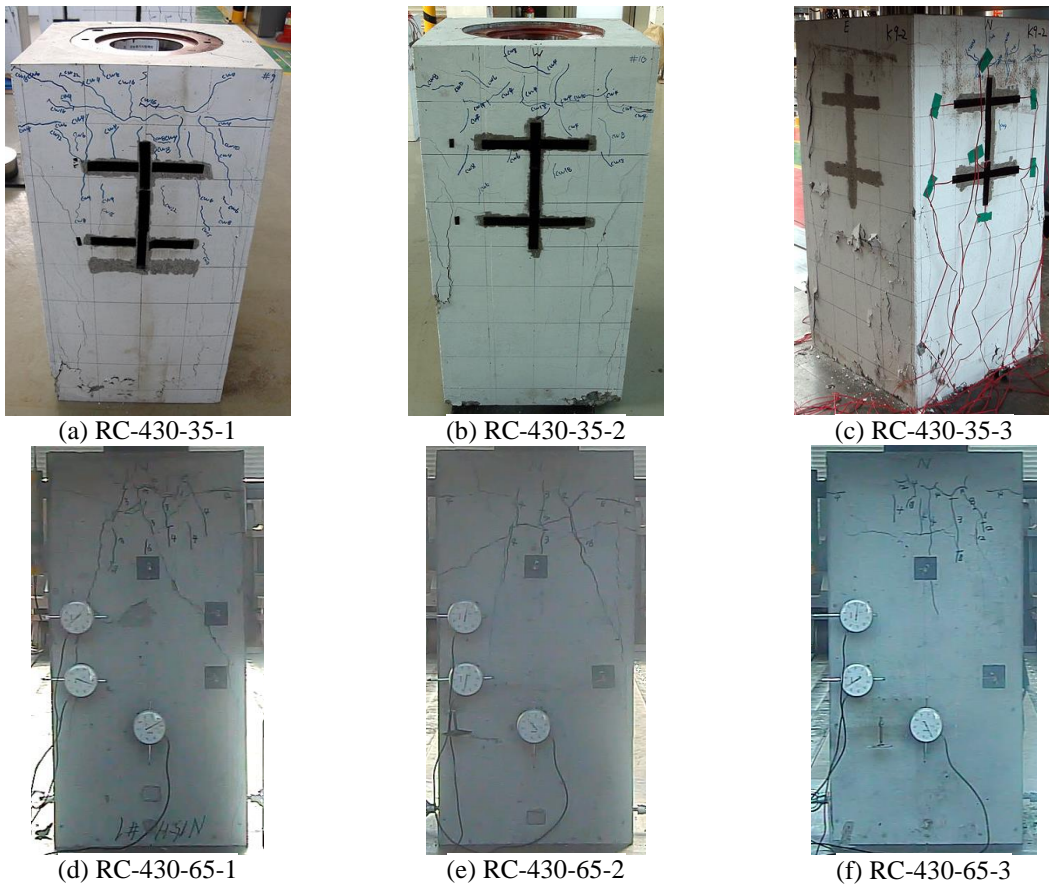


Fig. 9 Failure modes of specimens reinforced with only steel rebars

therefore prevent a bursting failure by splitting at the ultimate state.

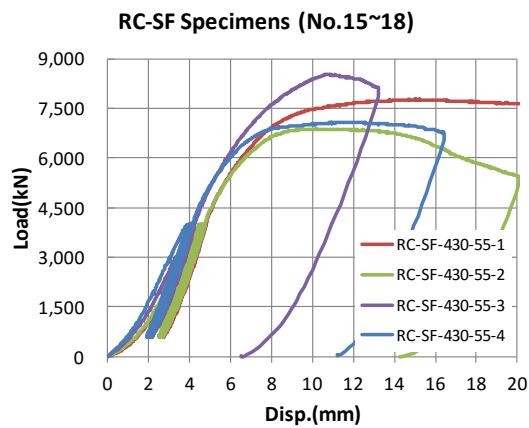


Fig. 10 Load-displacement curves of load-transfer tests for specimens reinforced with steel bars and steel fiber

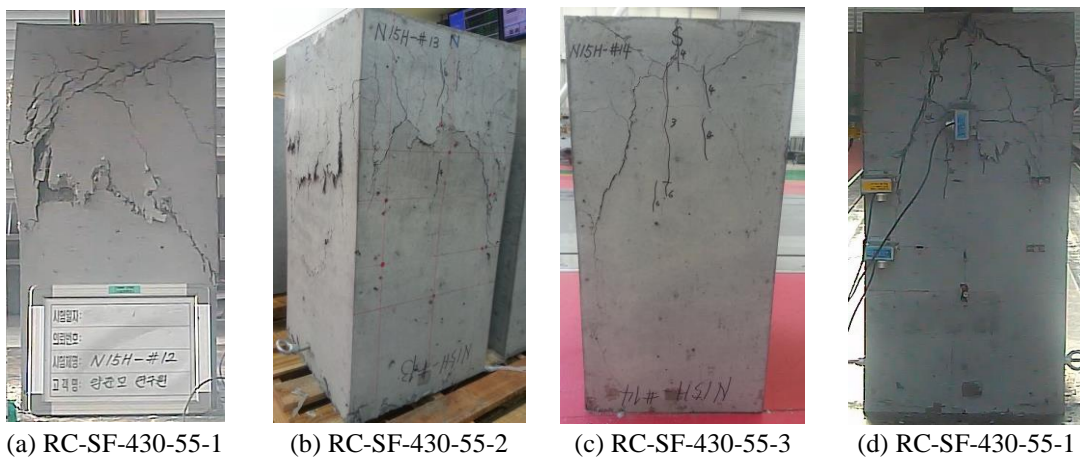


Fig. 11 Failure modes of specimens reinforced with only steel fiber

3.3 Specimens reinforced with steel rebars and steel fiber

Fig. 10 and Fig. 11 show the load-displacement curves of the load-transfer test and failure modes for the specimens reinforced with both steel rebars and steel fiber. Identical to the RCs trend, the ultimate strengths of the specimens RC-FSs are proportional to the confinement pressures; incidentally, a greater amount of ductile behavior was observed in the RC-SFs. The strength of RC-SF-430-55-3, with a confining pressure of 6.09 MPa (the highest in this group), is the highest, while the ductility of RC-SF-430-55-1, with a confining pressure of 5.83 MPa, is the highest; therefore, while the confining pressure affects the ultimate bearing strength, the impact of reinforcement details such as length, diameter, and the spacing of spiral rebars could be more relevant to ductility.

By comparison with specimens No. 13 and No. 14, specimens No. 15 and No. 16, which

comprise the same reinforcing details besides the steel-fiber addition, showed ultimate strengths that are 0.3% and 16% higher, respectively. In addition, the ductility, which is measured by the displacement difference that corresponds to the ultimate strength, of No. 15 is approximately 30 times higher, while No. 16 showed a 90% ultimate strength after the peak. The steel-fiber-reinforced concrete can therefore partially increase the strength and ductility of the anchorage when both steel fiber and steel rebars are used together and the equivalent flexural tensile strength is higher than 6.5 MPa; this capability is due to the greater toughness and post-peak behavior of steel-fiber-reinforced concrete. In these specimens, the failure of the concrete beneath the spiral, whereby a concrete cone that causes the splitting of the concrete below is formed, was observed. The addition of steel fiber could therefore avoid the complete crushing of the concrete.

4. Comparison with design equation

In the AASHTO LRFD Bridge Design specifications (2012), the bearing strength of an anchorage zone is strictly regulated by an allowable bearing stress, because, in many cases, the failure of post-tensioned members is governed by the bearing strength. The bearing strength (P_r) for the local anchorage zone with a basic anchorage device is taken as the following

$$P_{r,ASH} = \phi f_n A_b, \quad (2)$$

for which f_n is the lesser of the following

$$f_n = 0.7 f_{ci} \sqrt{\frac{A}{A_g}} \quad (3)$$

and

$$f_n = 2.25 f_{ci}, \quad (4)$$

where A is the maximum area of the portion of the supporting surface of the anchorage; A_g is the gross area of the bearing plate; A_b is the effective net area of the bearing plate including the bearing areas of the transverse ribs; and $\phi = 0.8$ is regarding the compression in the anchorage zones for which normal-weight concrete is used.

Special anchorage devices that do not satisfy the above requirements can be used, provided that they have been tested by an independent testing agency that is acceptable to the engineer, and they have met the acceptance criteria specified in Article 10.3.2 and Article 10.3.2.3.10 of AASHTO LRFD Bridge Construction Specification (2012); therefore, if the equation above is applied to a special anchorage with a sound spiral-rebar-confinement effect, a large underestimation of the ultimate bearing strength can be expected.

The effect of confinement on the ultimate bearing strength of the local anchorage zone was studied extensively by Roberts (1990), Sanders (1990). Roberts modified the classic work by Richart *et al.* (1928) to reflect the fact that the size and pitch of the spiral rebar that is typically used with anchorage devices do not produce the uniform confinement of the core concrete. She introduced the following strength-increment equation due to spiral-rebar confinement: $4.1 f_{lat} (1 - s/D_{sp})^2 A_{core}$. Roberts proposed an incorporation of both the confinement of the surrounding concrete (A/A_g ratio effect) and spiral-bar confinement for the ultimate load of the local zone, and a flat upper limit of 8.3 MPa. NCHRP Reports (1994) modified the prediction

equation for the ultimate strength of the anchorage zone for the special anchorage by introducing a calibration factor (η) that is based on the acceptance-test results. Typical values for η range from 0.85 to 0.95; in this study, 0.85 was assumed for η for the comparison between the test and the analysis results. The NCHRP Reports prediction equation is given by the following

$$P_{r,NCH} = \eta(P_c + P_s) \leq 3f_{ci} A_b, \quad (5)$$

$$P_c = 0.8f_{ci} \sqrt{\frac{A}{A_g}} A_b \leq 2f_{ci} A_b, \quad (6)$$

and

$$P_s = 4.1f_{lat} \left(1 - \frac{s}{D_{sp}}\right)^2 A_{core}. \quad (7)$$

Eq. (5) to Eq. (7) were developed based on the test results from the use of the basic anchorages and the special anchorages with a rib; however, the increased bearing area from the transverse ribs in the calculation of the effective net bearing area, A_b , was not considered for the formulation of these equations. As mentioned above, the failure mode of the anchorage zone is determined by the local reinforcement; furthermore, it also implies that the contribution of the transverse ribs regarding the ultimate bearing capacity may be affected by the reinforcement detail. When the confinement pressure on the concrete around the anchorage device is sufficient, it is expected that the contribution will increase, but it may become negligible in the other case. To quantify the effect of ribs, the ultimate bearing strength was calculated using Eq. (2) and Eq. (5). In each application of the design equation, the following two cases were considered: (1) ribs are considered in the calculation of the bearing area (A_b); (2) ribs are not considered in the calculation of the bearing area (A_b'). The prediction results and the ratio of the predictions to the test results can be found in Table 5.

4.1 Specimens reinforced with only steel fiber

As was predicted regarding the contribution of ribs toward the ultimate bearing strength, the Pr-1 and Pr-3 design equations overestimate the ultimate strength of the SFs specimens that do not have rebars by 36% and 65% on average, respectively, when ribs are considered; when ribs are not considered, AASHTO (Pr-2) and NCHRP (Pr-4) underestimate the ultimate strength by 33% and 18%, respectively. The implication here is that the addition of a steel fiber that provides an equivalent tensile strength of 2.8 MPa or less cannot contribute to the confinement of concrete. Consequently, the increase of the bearing area by the transverse ribs cannot be expected and it is appropriate to consider only the upper bearing-plate area when the ultimate bearing strength regarding an absence of rebar specimens is predicted. If the reinforcement is not installed, the difference between the two design equations is simply the coefficient value. Considering the reduction coefficient (Φ), the final coefficient values for AASHTO and NCHRP are 0.56 and 0.68, respectively. For this specimen group, the NCHRP for which the ribs are not considered provides a relatively more accurate prediction.

4.2 Specimens reinforced with only steel rebars

In contrast to the SFs specimens, the RCs specimens are underestimated by Pr-2 and Pr-4 to an extent that is too great when ribs are not considered. When the rib areas are considered, Pr-1

Table 5 Comparison between test results and predictions

No.	Specimens	Predicted strength (kN) / Ratio of predictions to tests (%)			
		$P_{r,ASH,Ab}$ (Pr-1)	$P_{r,ASH,Ab}$ (Pr-2)	$P_{r,NCH,Ab}$ (Pr-3)	$P_{r,NCH,Ab}$ (Pr-4)
1	SF-430-50-1	4,633 kN/99%	2,297 kN/49%	5,626 kN/121%	2,789 kN/60%
2	SF-430-50-2	4,085/110	2,026/54	4,960/133	2,460/66
3	SF-430-50-3	5,344/121	2,650/60	6,489/146	3,217/73
4	SF-430-50-4	4,580/136	2,271/67	5,562/165	2,758/82
5	SF-360-70-5	5,788/196	2,870/97	7,029/238	3,485/118
6	SF-360-70-6	5,325/143	2,640/71	6,466/174	3,206/86
7	SF-360-70-7	5,740/61	2,846/80	6,970/195	3,456/97
8	SF-360-70-8	5,325/173	2,640/86	6,466/210	3,206/104
Aver. / S.D. of Ratio (SFs)		136%/33%	67%/16%	165%/40%	82%/20%
9	RC-430-35-1	3,150 kN / 62%	1,562 kN/31%	5,213 kN/102%	3,285 kN/64%
10	RC-430-35-2	3,150/61	1,562/30	4,859/94	2,931/57
11	RC-430-35-3	3,289/57	1,631/28	5,643/98	3,630/63
12	RC-430-65-1	5,886/68	2,918/34	8,797/102	5,194/60
13	RC-430-65-2	5,886/76	2,918/38	8,305/107	4,702/61
14	RC-430-65-3	5,886/99	2,918/49	7,799/131	4,196/71
Aver. / S.D. of Ratio (RCs)		68%/15%	34%/8%	104%/13%	62%/5%
15	RC-SF-430-55-1	5,029 kN/65%	2,493 kN / 32%	7,264 kN / 93%	4,186 kN/54%
16	RC-SF-430-55-2	5,029/73	2,493/36	6,758/98	3,680/53
17	RC-SF-430-55-3	5,029/59	2,493/29	7,079/83	4,000/47
18	RC-SF-430-55-4	5,029/71	2,493/35	6,673/94	3,594/51
Aver. / S.D. of Ratio (RC-SFs)		66%/6%	33%/3%	92%/7%	51%/3%

underestimates the ultimate strengths by 32% on average, while Pr-3 overestimates them by 4% on average. For the RCs specimens that are reinforced with spirals and stirrups, the increase of the net bearing area through the transverse ribs contributes to the strength enhancement; consequently, it is suitable to consider the entire rib area for the prediction of the ultimate strength. If the rebar is installed, the additional difference between the two design equations according to AASHTO and NCHRP is the strength increase from the confinement of the concrete, which is expressed as Eq. (7). Comparisons between the average and standard deviation values of the prediction ratios and the test results confirm again that the Pr-3 of NCHRP estimates the strength more accurately. The largest difference between the prediction by Pr-3 of NCHRP and the test result is found in RC-430-65-3, of which the spiral-confinement pressure of 3.28 MPa is the lowest among the specimens. The average ratio obtained by Pr-3 for the high-strength specimens, RC-430-65s, is larger than RC-430-35s and 1.0.

These results reveal that NCHRP (Pr-3) overestimates the ultimate bearing strength for high-strength concrete specimens and its effect becomes greater when the spiral-confinement pressure decreases. It is possible to conclude that the NCHRP equation can be conservatively applied to various local anchorage zones for the prediction of the ultimate bearing strength by changing conditions such as a consideration of the rib area and the calibration factor. For the specimens

reinforced with less than 4 MPa of confining pressure, the additional bearing area from the transverse ribs is not considered; otherwise, this additional bearing area needs to be considered. Alternatively, a calibration factor (η) that is lower than that of the lower-strength-concrete specimen needs to be used for the high-strength-concrete specimen.

4.3 Specimens reinforced with steel bars and steel fiber

The results of RC-SFs are similar to those of RCs in that the specimens are underestimated by too much when ribs are not considered for AASHTO (Pr-2) and NCHRP (Pr-4). When considering the rib areas, the ultimate strengths are underestimated by 34% on average by AASHTO (Pr-1) and 8% on average by NCHRP (Pr-3). In the RC-SFs specimens, the ultimate strengths are not overestimated, even under the same rebar-reinforcement details; the reason here may be the addition of steel fiber that increases the equivalent flexural tensile strength to 6.5 MPa and provides additional confinement to the concrete. Through the addition of steel fiber, the 31% overestimation of RC-430-65-3 changes to a 2% underestimation of RC-SF-430-55-2, for which the rebar detail and the confinement pressure are the same as those of RC-430-65-3 when the Pr-3 is used. The addition of steel fiber can therefore enhance the rebar-confinement effect regarding concrete, even though it cannot replace all of the rebars. Also, the addition of steel fiber may help to avoid a congestion of the rebars in the anchorage zone to improve the workability; however, for its use in structural design, further tests and analyses and a quantification of its effect may be required.

5. Conclusions

In this paper, the effects of reinforcement with steel fiber and rebar on the ultimate bearing strength of the local anchorage zone was investigated, whereby experiments and comparisons between the test results and design-equation predictions served as the basis (AASHTO 2012, NCHRP 1994). Eighteen specimens were fabricated with the same anchorage device, which is one of the conventional anchorage devices, and two transverse ribs secured the additional bearing area for a compact anchorage-zone design. Eight specimens were reinforced with only steel fiber and are of two concrete strengths, while six were reinforced with only rebars for two concrete strengths. The other four specimens were reinforced with both rebars and steel fiber for a single concrete strength.

From the test and the comparison between the design-equation predictions and the test results, the following results were found:

- (1) A high ultimate bearing strength, or a load-transfer capacity from the anchorage to the concrete, can be achieved by using both high-strength concrete and a large amount of rebar reinforcement.
- (2) The relationship between the section efficiency and the amount of lateral reinforcement is positive, but it is negative between the former and the concrete strength.
- (3) Reinforcement details such as the depth of the spiral significantly impact the section efficiency.
- (4) The limit on the confining pressure depends on the rebar and steel-fiber reinforcements. It can be decreased with the aid of steel-fiber confinement.
- (5) The steel fiber alone cannot provide enough confinement and bursting capacity to the local

post-tensioning anchorage zone when the equivalent flexural tensile strength of the steel-fiber-reinforced concrete is less than 2.8 MPa; furthermore, there seems to be no relation between the ultimate strength of the load-transfer tests and the tensile properties of steel-fiber-reinforced concrete under this design condition. A confinement action due to steel fibers comparable to a spiral could be by extreme volumes of fibers, such as 3% or more.

(6) The failure mode of the SF specimens was observed as a split fracture and is governed by the bursting force. The RCs specimens failed by a complete crushing of the concrete at the local zone, or from the failure of the concrete beneath the spiral with the formation of a concrete cone that causes the splitting of the concrete below; the latter is also the cause of the failure of the RC-SFs. The addition of steel fiber could therefore avoid the complete crushing of the concrete.

(7) The toughness and post-peak behavior could be dramatically improved by the addition of steel fiber in the reinforced-concrete anchorage zone.

(8) For the SFs specimens, the NCHRP equation without a consideration of ribs provides a reasonable prediction.

(9) For the RCs specimens, the NCHRP equation can be conservatively applied to various local anchorage zones for the prediction of the ultimate bearing strength by changing conditions such as the consideration of the rib area and the calibration factor. For the specimens reinforced with less than 4 MPa of confining pressure, the additional transverse-rib bearing area is not considered; otherwise, this additional bearing area must be considered. Alternatively, a calibration factor (η) that is lower than that of the lower-strength-concrete specimen needs to be used for the high-strength-concrete specimen.

(10) For the RC-SFs specimens, the addition of steel fiber could enhance the rebar-confinement effect of concrete, even though it cannot replace all of the rebars, and the NCHRP equation for which the rib area is considered provides a reasonably accurate prediction.

Acknowledgments

This research was supported by a grant (13SCIPA01) from Smart Civil Infrastructure Research Program funded by Ministry of Land, Infrastructure, and Transport (MOLIT) of Korea government and Korea Agency for Infrastructure Technology Advancement (KAIA).

References

- AASHTO (American Association of State Highway and Transportation Officials) (2002), *Specifications for Highway Bridges*, 17th Edition, AASHTO, Washington D.C., USA.
- AASHTO (American Association of State Highway and Transportation Officials) (2010), *AASHTO LRFD Bridge Design Specifications*, AASHTO, Washington D.C., USA.
- ACI 318-14 (2014), *Building code requirements for structural concrete and commentary*, American Concrete Institute; Farmington Hills, MI, USA.
- ASTM C1609/C1609M-12 (2012), *Standard test method for flexural performance of fiber-reinforced concrete (using beam with third-point loading)*, ASTM International Standard Worldwide, West Conshohocken, PA.
- Breen, J.E. (1994), "Anchorage zone reinforcement for post-tensioned concrete girder", NCHRP Report 356, Transportation Research Board, Washington D.C., USA.

- Cervenka, V. and Ganz, H.R. (2014), "Validation of post-tensioning anchorage zones by laboratory testing and numerical simulation", *Struct. Concrete*, **15**(2), 258-268.
- EOTA (European Organisation for Technical Approvals) (2002), *ETAG 013: Guideline for European technical approval of post-tensioning kits for prestressing of structures*, EOTA, Brussels, Belgium.
- Guyon, Y. (1953), *Prestressed Concrete*, Wiley, NJ, USA.
- Kim, J.K., Seong, T.R., Jang, K.P. and Kwon, S.H. (2013), "Tensile behavior of new 2,200 MPa and 2,400 MPa strands according to various types of mono anchorage", *Struct. Eng. Mech.*, **47**(3), 383-399.
- KS D 3504 (2011), *Steel bars for concrete reinforcement*, Korean Standards Association, Seoul, Korea.
- KS D 7002 (2011), *Uncoated stress-relieved steel wires and strands for prestressed concrete*, Korean Standards Association, Seoul, Korea.
- Morgan, D.R., Mindess, S. and Chen, L. (1995), "Testing and specifying toughness for fiber reinforced concrete and shotcrete", *Proceedings of 2nd University - Industry Workshop on Fiber-Reinforced Concrete and Other Advanced Composites, Fiber-Reinforced Concrete - Modern Developments*, Toronto.
- PTI (Post-Tensioning Institute) (2006), *Post-Tensioning Manual*, 6th Edition, PTI.
- Richart, F.E., Brandtzaeg, A. and Brown, R.L. (1928), "A study of the failure of concrete under combined compressive stresses", Research Bulletin No. 185; Univ. of Illinois Engineering Experimental Station, USA.
- Roberts-Wollmann, C.L. (2000), "Design and test specifications for local tendon anchorage zones", *ACI Struct. J.*, **97**(6), 867-875.
- Roberts, C.L. (1990), "Behavior and design of the local anchorage zone of post-tensioned concrete members", Master's Thesis, University of Texas at Austin, USA.
- Sanders, D.H. (1990), "Design and behavior of anchorage zones in post-tensioned concrete members", Doctoral dissertation, University of Texas at Austin, USA.